

TWO-NUCLEON PION ABSORPTION IN ${}^4\text{He}$ AT 1 GeV/c

T. Nagae, T. Fukuda, M. Sekimoto, T. Miyachi, and P. Kitching^{a)}
Institute for Nuclear Study, University of Tokyo
Tanashi, Tokyo 188, Japan

I. Nomura
RIKEN
Wako, Saitama 351-01, Japan

I. Arai, K. Tomizawa, H. Kitayama^{b)}, Y. Nagasaka, S. Ueno, and K. Waki^{c)}
Institute of Physics, University of Tsukuba
Tsukuba, Ibaraki 305, Japan

K. Maeda, and T. Suda
College of General Education, Tohoku University
Sendai, Miyagi 980, Japan

H. Matsuyama^{d)}
Laboratory of Nuclear Science, Tohoku University
Sendai, Miyagi 980, Japan

T. Kobayashi^{e)}
National Laboratory for High Energy Physics (KEK)
Tsukuba, Ibaraki 305, Japan

D. Rowntree
Massachusetts Institute of Technology
Cambridge, MA 02139, USA

M.A. Prokhatilov, and V.I. Rasin
INR
Moscow, RU-117312, Russia

ABSTRACT

The first measurement of two-nucleon pion absorption in ${}^4\text{He}$ at 1 GeV/c has been performed at the KEK 12-GeV proton synchrotron. Both the (π^+ , pp) and (π^+ , pn) modes were measured and clearly identified, even at this energy. An isospin dependence was obtained which was different from that in the Δ -energy region.

(Submitted to Physics Letters B)

Since the 1970s, extensive theoretical and experimental studies on pion absorption

have been carried out, with most of the data coming from the meson factories: the beam energy has, however, been limited up to ~ 500 MeV [1]. In this energy region the $\Delta(1232)$ resonance plays an important role in the pion absorption mechanism at the doorway stage. The strong isospin dependence and incident energy dependence of the absorption cross sections have been well understood in terms of this mechanism.

Recently, much emphasis has been put on studies of multi-nucleon absorption (absorption by more than two nucleons) using helium isotopes [2]. Substantial amounts of multi-nucleon absorption have been reported at higher energies above the Δ -energy region. A theoretical estimate [3] of the energy dependence of multi-nucleon absorption predicts the dominance of this mechanism over two-nucleon absorption at higher energies. For two-nucleon absorption cross sections on ${}^3\text{He}$, scaling according to quasi-deuteron (a nucleon pair with $T=0$) counting holds well in the Δ -energy region; i.e., the cross section is 1.5- times that for $\pi^+ + d \rightarrow 2p$ and the angular distribution also agrees well. However, a small enhancement of the cross section has been reported above the Δ resonance [4,5]. At 1 GeV/c, there is no reason to assume the dominance of absorption on $T=0$ nucleon pairs, since the effect of the Δ -resonance is not prominent at this energy. Therefore, a measurement of the isospin dependence of two-nucleon absorption above 500 MeV is of great initial importance to investigate the reaction mechanism.

An experiment (E217) was performed at the π^2 beam line of the KEK 12-GeV proton synchrotron (PS) between April and December, 1990.

Figure 1 shows a schematic view of the experimental setup. To cover wide forward angles, two different setups were used. The incident beam comprised positive pions having a momentum of 1 GeV/c ($\Delta p/p=1.5\%$) with a typical intensity of $10^5/\text{spill}$, which was defined with four sets of scintillation counters (S0-3). The S0 counter was located about 13 m upstream of the target position, and was used to reject protons with time-of-flight (TOF) information in the fast trigger. Positrons in the beam

^{a)} and also, University of Alberta, Edmonton, AB, T6G 2N5, Canada and TRIUMF, Vancouver, BC, V6T 2A3, Canada.

^{b)} Present address: UL VAC Japan Ltd., Chigasaki, Kanagawa 253, Japan.

^{c)} Present address: JR, Tokyo, Japan.

^{d)} Present address: Toshiba Co., Kawasaki, Kanagawa 210, Japan.

^{e)} Present address: RIKEN, Wako, Saitama 351-01, Japan.

were identified with a gas Cherenkov counter in an offline analysis. Contamination of muons in the pion beams was estimated to be 4.0% based on a calculation using the computer code DECAY TURTLE. The incident angles and positions were traced with two sets of MWPCs (BDC1, 2) having a wire spacing of 1 mm. The horizontal beam divergence was about ± 15 mrad. As a target, ^4He was chosen because the effect of the final-state interaction would be small and the two-nucleon absorption events could be easily extracted. Liquid ^4He of 2.8 g/cm^2 was filled in a cylindrical container made of stainless steel with a window thickness of 0.5 mm.

A dipole magnet with an aperture of $82 \text{ cm}[\text{V}] \times 40 \text{ cm}[\text{H}] \times 70 \text{ cm}[\text{L}]$ and a magnetic field of 1.2 T was used to analyze the momentum of the forward-scattered particles. A track was detected by five sets of drift chambers (FDC1-5) with a position resolution of $\sim 300 \mu\text{m}$ for each plane. The particles were identified with a TOF wall (FH1-9), which comprised nine plastic scintillators having a size of $20 \times 150 \times 3 \text{ cm}^3$. The particles with momenta $> 0.6 \text{ GeV}/c$ within an angular range from 5 to 35° were accepted in the forward spectrometer, which was sufficiently wide to measure not only the high-momentum protons ($> 1.3 \text{ GeV}/c$) from two-nucleon absorption, but also other low-momentum particles from various background processes.

In the backward region ($80^\circ - 170^\circ$) we had two TOF walls (NHA and NHB) with veto counters (VA and VB, respectively) for charged particles. In these walls both protons and neutrons were detected, and the particle velocities were measured based on the TOF with a time resolution of about 400 psec (rms). The NHA was the same TOF counter wall as that used for E173 [6] without any back-side and left-side veto counters. Based on a Monte-Carlo calculation, it was found that the detection efficiency for neutrons from $400 \text{ MeV}/c$ to $950 \text{ MeV}/c$ was enhanced to be $11 \pm 1\%$. It comprised five layers of 3-cm thick, 20-cm wide, plastic scintillators in ten rows. The NHB comprised seven plastic scintillators having a size of $20 \times 10 \times 150 \text{ cm}^3$, of which the detection efficiency for the neutrons in the same momentum range was estimated by a Monte-Carlo simulation to be $10 \pm 1\%$.

A veto counter (BV) used to reject beam particles without any reactions in the target was placed downstream of the target. The trigger condition for the data taking was chosen with the coincidence condition of $\text{BEAM} \cdot \overline{\text{BV}} \cdot \text{FH} \cdot (\text{NHA} + \text{NHB})$.

For forward-going particles, we clearly identified π^+ 's, protons and deuterons based on their momenta and TOFs. The overall detection efficiency of the forward spectrometer was estimated to be $59 \pm 3\%$ for high-momentum protons, which was mainly limited by the detection efficiencies of the five tracking chambers.

For backward-emitted particles, we could only measure the velocities of the particles. For a flight-path correction, a reaction point was obtained as a crossing point between an incident track and a forward track, of which the resolution ($< 6 \text{ mm}$) was much less than the scintillator thickness of the TOF counters. Taking into account kinematical correlations, we could classify the observed events, as shown in Fig. 2(a). In this figure, the scatter plot between the momenta of the forward protons identified and the particle velocities measured in one of the TOF hodoscopes is shown. In the high-momentum side ($> 1.3 \text{ GeV}/c$) and low-velocity region ($0.4 - 0.7$), a cluster of two-nucleon absorption events is seen. Another cluster of events in the high-velocity (< 0.8) region with protons of around $1.1 \text{ GeV}/c$ would correspond to a quasi-elastic scattering of pions in the backward direction ($\pi^+ p \rightarrow p^+ \pi$). With a velocity cut of 0.7 , we can reject most of the pions coming from this process. The momentum resolution of the TOF hodoscopes was $2 - 5\%$ for nucleon velocities of $0.4 - 0.7$.

To select two-nucleon absorption events, we first selected those events with one proton in the forward spectrometer and one slow nucleon in the backward hodoscope. Then, the events were selected with cuts on the transverse momentum sum of two nucleons and the missing mass of two absorbing nucleons ($\sqrt{(\vec{p}_1 + \vec{p}_2 - \vec{p}_\pi)^2}$; \vec{p}_i denotes the four momentum of the i -th nucleon), taking account of the momentum resolutions. In Fig. 2(b), the missing-mass distribution is shown, in which the peak at around $1.8 \text{ GeV}/c^2$ corresponds to the two-nucleon absorption. After the selection, a differential cross section for each forward angle was obtained by integrating the

backward angular distribution with one Gaussian and the background distributions: the background contribution, which might come from three-nucleon absorption etc., was found to be less than 10%. In the very forward angles we integrated the extrapolated data to the outside of the backward hodoscopes' coverage.

In Fig. 3, the differential cross sections are shown for the (π^+, pp) and (π^+, pn) modes on ${}^4\text{He}$. As a reference, the $\pi^+d \rightarrow 2p$ data at 1 GeV/c [7] are shown. Although the angular range shown is limited up to ~ 53 degrees in the center-of-mass system, the integrated cross section of $\pi^+d \rightarrow 2p$ in this range is almost 72% of the total cross section.

One remarkable thing is that the angular distributions of ${}^4\text{He}(\pi^+, pn)$ and $\pi^+d \rightarrow 2p$ are quite different, i.e., that of ${}^4\text{He}(\pi^+, pn)$ is much more forward peaked. By counting the number of nucleon pairs in ${}^4\text{He}$, the (π^+, pp) cross section could be expressed based on the cross sections on nucleon pairs in different initial isospins as follows:

$$\sigma({}^4\text{He}(\pi^+, pp)) = N_1\sigma_1 + N_0\sigma_0,$$

where $\sigma_i(N_i)$ denotes the absorption cross section on the nucleon pair (the number of nucleon pair(s) with isospin i). For the deuteron case, however, only σ_0 contributes to the (π^+, pp) cross section. If we assume that the (π^+, pn) cross section has only the $T=1$ pair in the final state, it is equal to σ_1 . Thus, the (π^+, pp) cross section on ${}^4\text{He}$ could be expressed as $\sigma({}^4\text{He}(\pi^+, pp)) = N_1\sigma({}^4\text{He}(\pi^+, pn)) + N_0\sigma_d(\pi^+, pp)$. In Fig. 3, the result of fitting with $N_0=2.35 \pm 0.4$ (statistical) ± 0.5 (systematic) and $N_1=1$ (fixed) is indicated by the solid line, which reproduces the data quite well. The obtained N_0 value is slightly smaller than that (~ 3.0) in the Δ -energy region [8] to 500 MeV [9], while a 30-40% suppression was reported at 114 and 162 MeV [10].

To determine the isospin dependence we calculated the cross section ratio of $\sigma({}^4\text{He}(\pi^+, pn))/\sigma_d(\pi^+, pp) = 0.56 \pm 0.16$ (statistical) ± 0.13 (systematic),

where $\sigma({}^4\text{He}(\pi^+, pn))$ is the cross section between 0 and 35 degrees (in Lab.); so that this ratio gives a lower limit. At 120 MeV [8], the ratio $\sigma({}^4\text{He}(\pi^+, pn))/\sigma_d(\pi^+, pp)$, which can be directly compared to $\sigma({}^4\text{He}(\pi^+, pn))/\sigma_d(\pi^+, pp)$, is 0.15 ± 0.04 . Since only one $T=1$

nucleon pair contributes to the cross section in both ${}^4\text{He}(\pi^+, pn)$ and ${}^3\text{He}(\pi^+, pn)$, our value could also be compared with the cross-section ratio of $\sigma({}^3\text{He}(\pi^+, pn))/\sigma_d(\pi^+, pp)$, which is ~ 0.1 from 62.5 to 206 MeV [4, 11]; while a large value of ~ 0.6 was reported at 350 MeV [12].

In summary, the first experiment concerning pion absorption at 1 GeV/c has been carried out at KEK-PS on a ${}^4\text{He}$ target. To extract the isospin dependence of the two-nucleon absorption, both the ${}^4\text{He}(\pi^+, pp)$ and ${}^4\text{He}(\pi^+, pn)$ modes were measured. An enhancement of the cross section ratio of $\sigma({}^4\text{He}(\pi^+, pn))/\sigma_d(\pi^+, pp)$ was obtained in contrast to $\sigma({}^4\text{He}(\pi^+, pn))/\sigma_d(\pi^+, pp)$ and $\sigma({}^3\text{He}(\pi^+, pn))/\sigma_d(\pi^+, pp)$ in the Δ -energy region. Further, there exists a large difference in the angular distributions between ${}^4\text{He}(\pi^+, pn)$ and ${}^4\text{He}(\pi^+, pp)$, which suggests that different reaction mechanisms are involved in these reactions.

We would like to thank the staff members of KEK for supporting our experiment and Professor K. Nakai for his stimulating discussions. T.N. is grateful to Professor S. Homma for his continuous encouragement. We also express our thanks to Professor D. Ashery for his fruitful discussions concerning the interpretation of our data. Finally, it is our pleasure to thank Professor Y. Akaiishi for initiating our experiment through valuable discussions.

References

- [1] D. Ashery and J.P. Schiffer, *Ann. Rev. Part. Nucl. Sci.* 36 (1986) 207.
- [2] H. Weyer, *Phys. Rep.* 195 (1990) 295.
- [3] E. Oset, Y. Futami and H. Toki, *Nucl. Phys. A*448 (1986) 597.
- [4] P. Weber et al., *Nucl. Phys. A*501 (1989) 765.
- [5] L.C. Smith et al., *Phys. Rev. C* 40 (1989) 1347.
- [6] J. Chiba et al., *Phys. Rev. Lett.* 67 (1991) 1982.
- [7] M. Akemoto et al., *Phys. Lett.* 149B (1984) 321.
- [8] M. Steinacher et al., *Nucl. Phys. A*517 (1990) 413.
- [9] L.C. Smith et al., *Phys. Rev. C* 48 (1993) R485.
- [10] F. Adimi et al., *Phys. Rev. C* 45 (1992) 2589.
- [11] K.A. Aniol et al., *Phys. Rev. C* 33 (1986) 1714.
- [12] L.C. Smith et al., A contributed paper to PANIC Conf., Kyoto, Japan, 1987.

Figure Captions

Fig. 1 Schematic view of the experimental setup of E217. Two different setups are superimposed.

Fig. 2 (a) Scatter plot between the momentum of the forward protons and the velocity of the backward particles ($\theta_{\text{FWD}}=15^\circ-18^\circ$).

(b) Typical example ($\theta_{\text{FWD}}=25.5^\circ-28.5^\circ$) of the missing-mass distribution of two absorbing nucleons ($\sqrt{(\vec{p}_1 + \vec{p}_2 - \vec{p}_x)^2}$; \vec{p}_i denotes the four momentum of the i -th nucleon). The shaded area is selected as the two-nucleon absorption component.

Fig. 3 Angular distributions of the (π^+ , pp) and (π^+ , pn) cross sections on a ^4He target at 1 GeV/c with reference to the (π^+ , pp) cross section for a deuteron (a dashed line is only to guide the eye). The error includes statistical one and systematic ones due to background subtraction. Regarding the solid line, see the text.

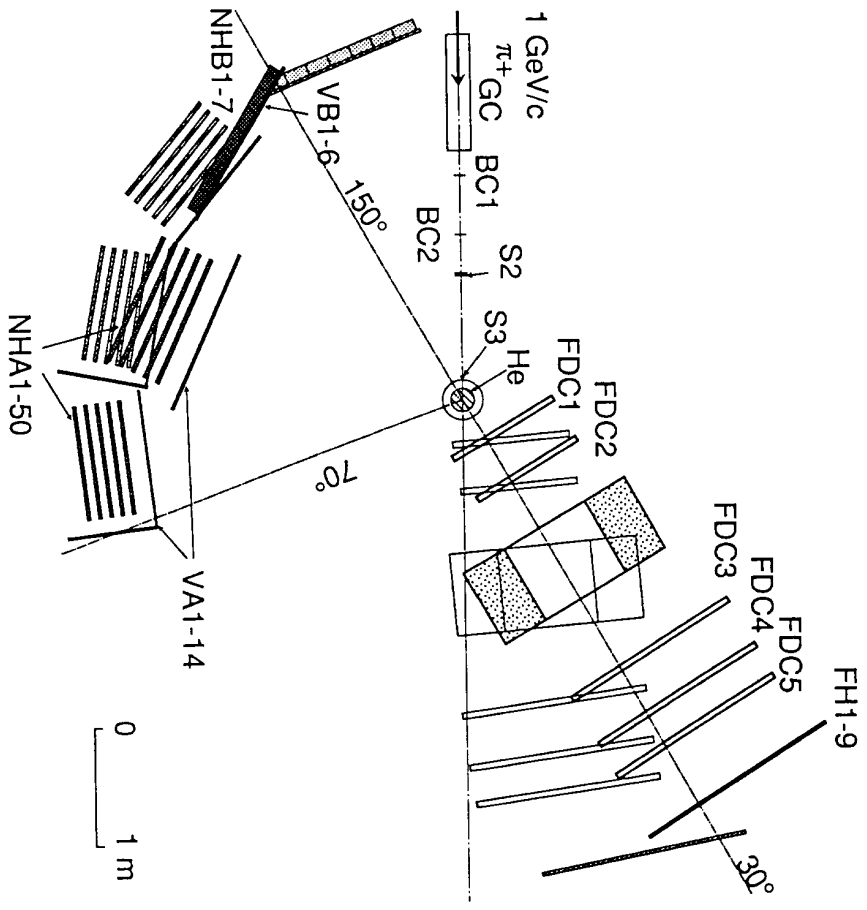


Fig. 1

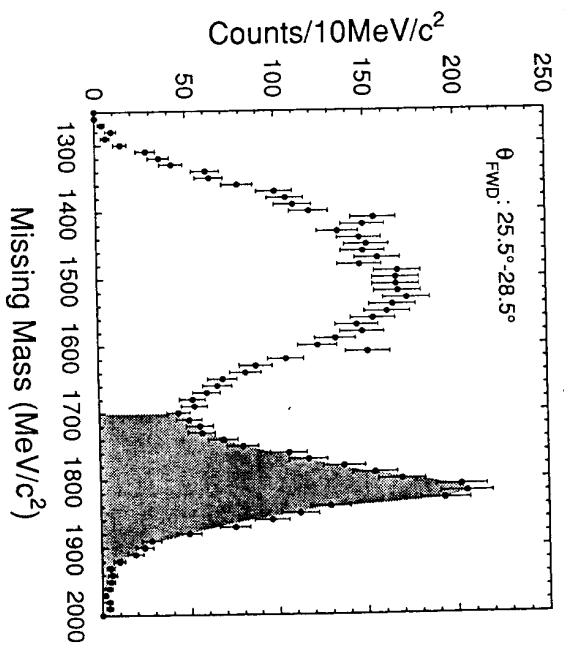
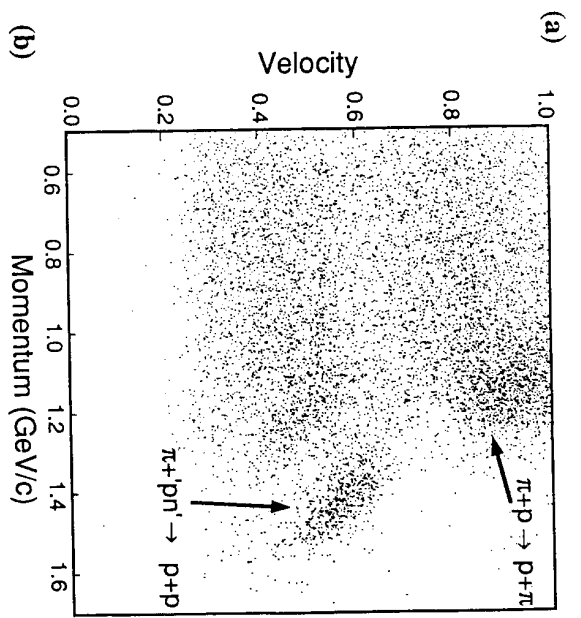


Fig. 2

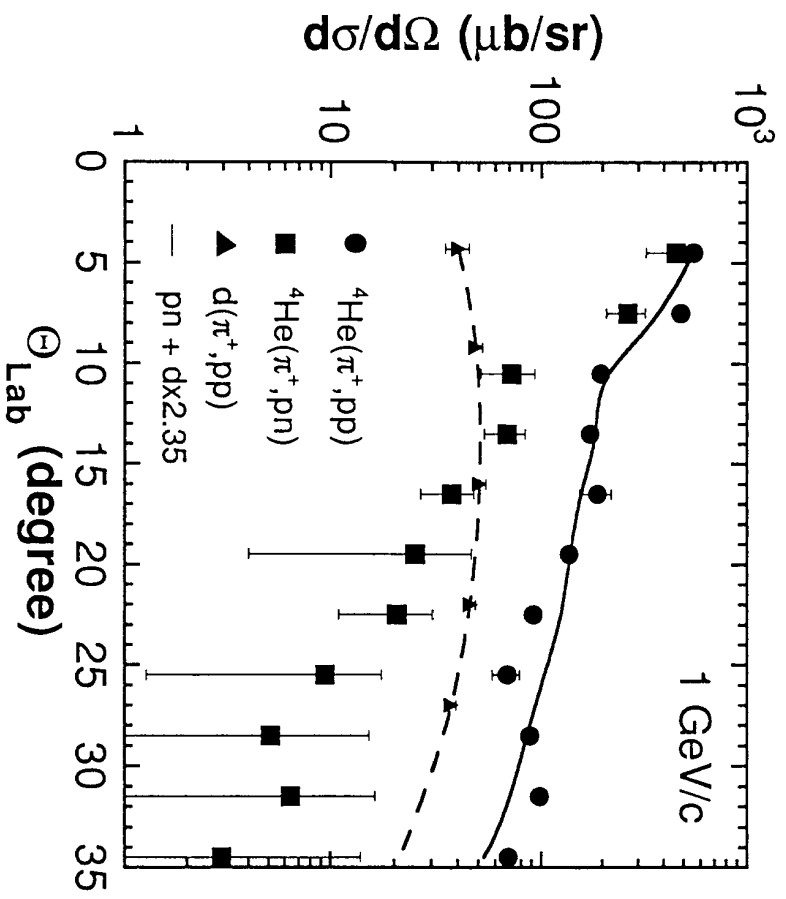


Fig. 3